ORGANOMETALLICS

Article

pubs.acs.org/Organometallics

Yttrium-Catalyzed Amine−Silane Dehydrocoupling: Extended Reaction Scope with a Phosphorus-Based Ligand

Adi E. Nako, Wenyi Chen, Andrew J. P. White, and Mark R. Crimmin*

Department of Chemistry, Imperial College London, South Kensington SW7 2AZ, U.K.

Supporting Information

ABSTRACT: The scope of the catalytic dehydrocoupling of primary and secondary amines with phenylsilanes has been investigated using [Y{N(SiMe$_3$)$_2$}$_3$] and a four-coordinate analogue bearing a cyclometalated phosphonium methylide ligand. Inclusion of the phosphorus-based ligand on yttrium results in increased substrate scope in comparison to the tris(amide) analogue. While reversible C−H bond activation of the cyclometalated ligand was observed in stoichiometric experiments, D-labeling experiments and DFT calculations suggest that reversible ligand activation is not involved in silazane formation under catalytic conditions. We suggest that the extended reaction scope with the four-coordinate yttrium phosphonium methylide complex relative to the three-coordinate yttrium (tris)amide complex is a result of differences in the ease of amine inhibition of catalysis.

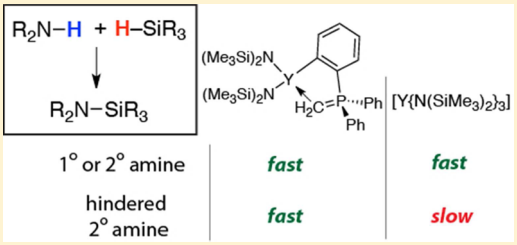

INTRODUCTION

The dehydrocoupling of amines and silanes to form silazanes is a reaction that has received considerable attention over the last 5 years.[1] While early investigations into silazanes focused on the formation of polysilazanes and their pyrolysis to form silicon nitride (Si_3N_4),[2] in recent years the Si−N moiety has found extensive use as a protecting group in organic synthesis or as part of kinetically stabilizing ligands in coordination chemistry.[3,4] Catalysts based upon elements from across the periodic table have been reported to effect the cross-dehydrocoupling of amines and silanes. Although catalysts incorporating Pt,[5] Rh,[6] Ru,[7] Ti,[8] Cu,[9] and U[10] along with those based on Lewis acids[11] and Lewis bases[12] have been known for some time, recently amide and alkyl complexes of the s-block and rare-earth elements have emerged as highly efficient and inexpensive mediators of this reaction.

For example, in 2007 Harder and co-workers reported that the dehydrocoupling of amines and silanes could be efficiently catalyzed by [(η^2-Ph$_2$CNPh)M(HMPA)$_3$] (M = Ca, Yb).[13a] Sadow and co-workers demonstrated improved reaction selectivity and scope through use of the magnesium complex [{To^M}MgMe] (To^M = tris(4,4-dimethyl-2-oxazolinyl)-phenylborate).[13b] Bis(amide) and bis(alkyl) complexes of Ca, Sr, Ba, and the related divalent lanthanide Yb, including [M{N(SiMe$_3$)$_2$}$_2$] (M = Ca, Sr, Ba) and [(IMes)Yb{N(SiMe$_3$)$_2$}$_2$] (IMes = 1,3-bis(2,4,6-trimethylphenyl)imidazol-2-ylidene) have been reported as catalysts for Si−N bond formation by the groups of Hill, Cui, and Carpentier.[13,14] The turnover frequency and turnover number for one of the most active barium catalysts, [Ba{CH(SiMe$_3$)$_2$}$_2$(THF)$_3$], reach 3600 h^{-1} and 396, respectively, for the dehydrocoupling of pyrrolidine and triphenylsilane.[13d] Divergent mechanistic arguments have materialized from these studies. Depending on the catalyst, it has been proposed that Si−N bond formation occurs through either a concerted σ-bond metathesis step between M−N and Si−H bonds or by nucleophilic attack of the nitrogen atom of a metal amide onto the electrophilic Si center to generate a hypervalent silicate intermediate that then decomposes through hydrogen elimination.[13,14]

We recently introduced the cyclometalated complex **1**. This complex incorporates the three elements of ligand design outlined in Figure 1—namely appended X- and L-type ligands

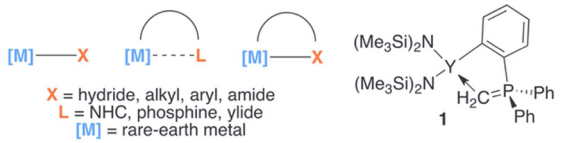

Figure 1. Catalyst design for small molecule activation with rare-earth metals.

along with reactive σ-bonded substiuents.[15] Here we show that **1** is a highly effective catalyst for the dehydrocoupling of amines and silanes. The inclusion of the phosphonium methylide ligand on yttrium results in an increase in the scope and efficiency of catalysis relative to the parent tris(amide) complex [Y{N(SiMe$_3$)$_2$}$_3$] (**2**).

Substrate activation through a reversible reaction of a chelating ligand has long been considered in the organometallic chemistry of the rare-earth elements. For example, the potential for cyclopentiadienyl systems to undergo reversible ligand activation has been appreciated since the early studies of Watson, Bercaw, and others on the addition of H−H and C−H and bonds to [(Cp*)$_2$M(Me)] (M = Lu, Sc).[16−18] This observation of ligand-based reactivity is not limited to tuck-in

Received: July 14, 2015
Published: August 20, 2015

DOI: 10.1021/acs.organomet.5b00607
Organometallics 2015, 34, 4369−4375

complexes or related species bearing appended X-type ligands: in 2010, Arnold and Turner reported the 1,2-addition of E−X (E = Si, Sn, P, B; X = Cl, N_3) bonds across the M−C bond of N-heterocyclic carbene adducts of scandium, yttrium, cerium, and uranium, along with elimination and subsequent carbon−heteroatom and nitrogen−heteroatom bond formation from isolated zwitterionic intermediates.[19] Parallels may be drawn with frustrated Lewis pairs based on zirconium and yttrium reported by Wass and co-workers.[20] Broadly both systems could be classified as a reactive metal with an appended L-type ligand (Figure 1).

As part of the current contribution, we have investigated the potential of **1** to react with substrates by reversible ligand activation under both stoichiometric and catalytic conditions. Although substrate activation by participation of *both* the appended L- and X-type ligands is possible under stoichiometric conditions, through the isolation of catalytic intermediates, D-labeling experiments, inhibition experiments, and DFT calculations, we conclude that reversible ligand activation is not involved in silazane formation under catalytic conditions. The extended reaction scope of catalyst **1** with respect to catalyst **2** is rationalized through a mechanism in which amine inhibition is more significant for the three-coordinate tris(amide) **2** than for the four-coordinate complex **1**.

RESULTS

Reaction Scope. The selective dehydrocoupling of $^{i}Pr_2NH$ and $PhSiH_3$ may be catalyzed by 5 mol % $[Y\{N(SiMe_3)_2\}_3]$ (**2**), producing $^{i}Pr_2NSiH_2Ph$ in 93% conversion after 164 h at 80 °C in C_6D_6.[7,8] Upon modification of the precatalyst to **1**, preparations proceed to high conversion within 24 h at 25 °C. Control experiments with **2** or mixtures of **2** and Ph_3PCH_2 revealed only trace formation of $^{i}Pr_2NSiH_2Ph$ after weeks at 25 °C (Scheme 1).

Scheme 1. Catalytic Dehydrocoupling of Diisopropylamine with Phenylsilane

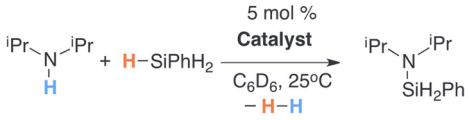

Catalyst	Time (h)	Yield (%)
1	26	86%
2	70	< 1%
2 + CH_2PPh_3	221	< 1%

On the basis of this observation we investigated **1** and **2** as catalysts for the cross-dehydrocoupling of a series of amines and silanes. The catalysts are selective for the 1:1 reaction of a number of primary and secondary amines with a series of organosilanes. The reaction scope along with a comparison of the two precatalysts is presented in Table 1. The products have been characterized by ^{1}H, ^{29}Si, ^{15}N, and ^{13}C NMR spectroscopy (see the Supporting Information).

Catalysts **1** and **2** show comparable activities for the addition of primary amines and unhindered secondary amines to phenylsilane and diphenylsilane. For example, comparison of the initial rates of the reaction of piperidine with diphenylsilane

Table 1. Reaction Scope of Amine−Silane Dehydrocoupling Catalyzed by 1 or 2

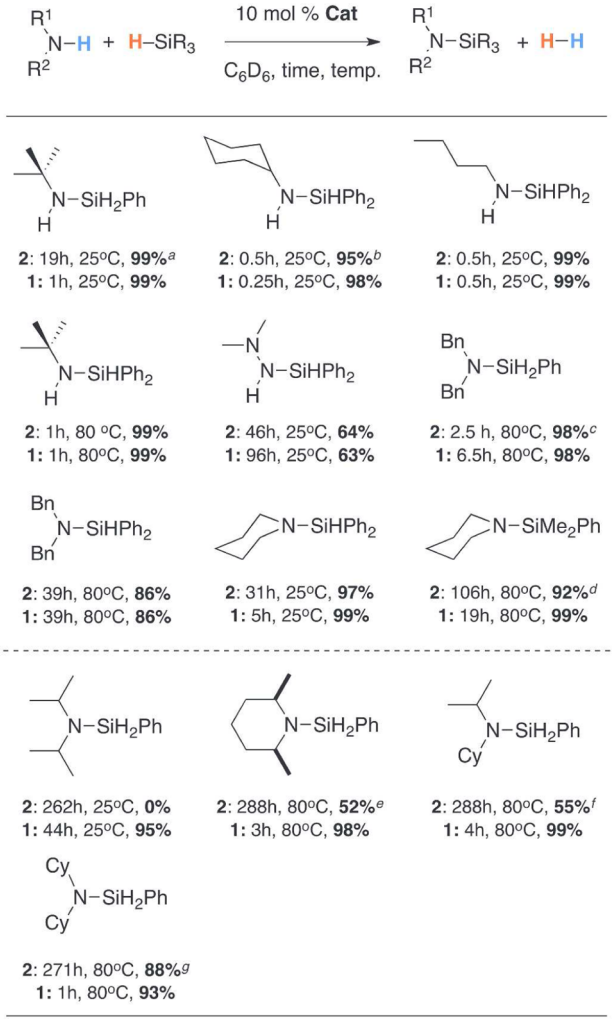

Reactions conducted with a 1:1 mixture of silane and amine. Yields were recorded by ^{1}H NMR spectroscopy against hexamethylbenzene or ferrocene as an internal standard. [a]57% after 2 h. [b]83% after 0.25 h. [c]80% after 2.5 h. [d]60% after 19 h. [e]17% after 21 h. [f]22% after 19 h. [g]12% after 19 h.

reveals near-identical activities for both catalysts with no observable induction period for either (Figures S1 and S2, in the Supporting Information). A handful of catalytic systems are known to be competent for the dehydrocoupling of sterically demanding secondary amines with silanes.[13,14] It is for these substrates that stark differences are noted for catalysts **1** and **2**. While **1** rapidly dehydrocouples dicyclohexylamine, 2,6-dimethylpiperidine, and isopropylcyclohexylamine with phenylsilane either at 25 °C or within a few hours at 80 °C, catalyst **2** is either inactive or requires more than 1 week at 80 °C to reach moderate to acceptable yields of the corresponding silazanes.

Catalyst Resting States. The *J* coupling between ^{89}Y and ^{31}P nuclei observed in NMR offers a useful spectroscopic handle to investigate the catalytic resting states. Monitoring catalytic preparations by $^{31}P\{^{1}H\}$ and ^{1}H NMR allowed the identification of two distinct regimes that are dependent on the amine employed. For sterically unhindered primary amines such as *N,N*-dimethylhydrazine, *n*-butylamine, and cyclohexylamine (regime 1, Table 1, top), free CH_2PPh_3 and varying

DOI: 10.1021/acs.organomet.5b00607
Organometallics 2015, 34, 4369−4375

amounts of $HN(SiMe_3)_2$ are observed by ^{31}P and ^1H NMR spectroscopy within the first 15 min of the reaction, suggesting facile protonolysis and displacement of the ylide from the coordination sphere of the catalyst. Similarly, for piperidine and *tert*-butylamine, **1** is consumed within the first point of analysis, in this case generating the corresponding triphenylphosphonium methylide adducts **3a,b** (Scheme 2).

Scheme 2. Synthesis of Catalyst Resting States 3a,b

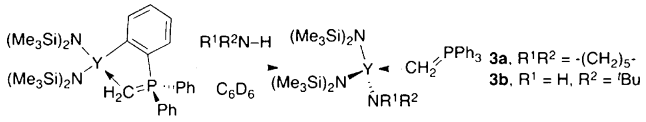

A stoichiometric reaction between **1** and piperidine in C_6D_6 resulted in clean formation of the in situ observed product. The reaction still occurs rapidly when **2**, Ph_3PCH_2, and excess amine (1.2 equiv) are dissolved in C_6D_6. Scale-up of this and a related reaction using *tert*-butylamine gave **3a,b** as crystalline solids in 50% and 69% yields, respectively (Scheme 2). The ^1H NMR spectra of **3a,b** both show a distinct sharp doublet of doublets for the methylide hydrogens (**3a**, δ 1.20 ppm, $^2J_{^{31}P-^1H}$ = 17.6 Hz, $^2J_{^{89}Y-^1H}$ = 2.4 Hz; **3b**, δ 1.13 ppm, $^2J_{^{31}P-^1H}$ = 17.6 Hz, $^2J_{^{89}Y-^1H}$ = 2.4 Hz). For **3b** the N−H resonance can be seen as a doublet at δ 2.18 ppm (1H, $^2J_{^{89}Y-^1H}$ = 2.4 Hz). The coupling to ^{89}Y was confirmed by running a $^1H\{^{31}P\}$ experiment. A single phosphorus environment was detected in each case (**3a,** δ +32.4 ppm, $^2J_{^{89}Y-^1H}$ = 5.0 Hz; **3b**, δ +32.5 ppm, $^2J_{^{89}Y-^1H}$ = 4.9 Hz). Single-crystal X-ray diffraction experiments confirmed the structures (Figure 2). The Y−C bond lengths in **3a** (2.5441(18) Å), **3b** (2.531(2) Å), and **2**·CH_2PPh_3 (2.554(3) Å) (vide infra) are within experimental error of one another.

Complex **3a** proved kinetically competent for the dehydrocoupling of piperidine and diphenylsilane at an initial rate similar to those of **1** and **2**. Similarly, **3b** was found to be catalytically competent for the reaction of phenylsilane and *tert*-butylamine, giving the corresponding silazane in 99% yield after 1 h at 25 °C. On the basis of this observation and the data presented in Table 1, we propose that for the addition of 1° amines and unhindered 2° amines to arylsilanes a common catalyst may be generated. Complexes **1**, **2**, and **3a,b** give rise to similar species under catalytic conditions. Hence, protonolysis of **2** with 1 equiv of amine yields observable intermediates **3a,b** that may lose 1 equiv of ylide and generate species similar to those derived from **1** under catalytic conditions.

During preparations of **1** we identified the ylide adduct **2**·CH_2PPh_3 (δ +30.5 ppm, C_6D_6) as an intermediate. Consistent with the hypothesis outlined above, VT NMR studies on isolated samples of **2**·CH_2PPh_3 in toluene-d_8 demonstrated that ylide coordination is reversible, with the equilibrium lying toward **2** + CH_2PPh_3 at higher temperatures (Figure 3).

In contrast when hindered secondary amines are employed as substrates (regime 2, Table 1, bottom), ring opening of the P-based ligand of **1** or displacement of the ylide from yttrium is not observed. For diisopropylamine, dicyclohexylamine, isopropylcyclohexylamine, and *cis*-2,6-dimethylpiperidine, **1** (δ +28.3 ppm) is observed as the catalyst resting state throughout the reaction. It is for these substrates that a significant difference between the activities of **1** and **2** is recorded in catalytic silazane formation (Table 1).

Reversible Ligand Activation under Stoichiometric Conditions. In order to probe whether the reaction of **1** with amines could be reversible, a series of deuterium labeling experiments were conducted. The reaction of $^tBuND_2$ with either **1** or **3b** resulted in significant D incorporation into the C−H bonds of *both* the methylide position and the aryl ring, as evidenced by ^1H and ^2H NMR spectroscopy (Scheme 3). A similar labeling experiment in which **1** was reacted with excess $^iPr_2ND$ neither led to ring opening of the phosphonium methylide ligand nor resulted in significant D incorporation into the aryl ring. This experiment is consistent with the observation of **1** as a catalytic resting state during the dehydrocoupling of $^iPr_2NH$ with $PhSiH_3$. In both labeling experiments D incorporation was observed into the methylide position, and control experiments in which triphenylphosphonium methylide was reacted with $^tBuND_2$ show facile H/D exchange between the N−D and C−H groups. As such, little mechanistic information can be gained from D incorporation into the methylide position of complexes **1** and **3b**.

The experiments were supported by DFT calculations using a sterically unhindered model. The addition of the N−H bond of dimethylamine across the Y−C_{ylide} and aryl Y−C_{Aryl} bonds of **A-1** (a model of **1** in which the −$N(SiMe_3)_2$ ligands have been replaced with NMe_2) is represented in Figure 4. Both reactions were found to occur by an energetically accessible σ-bond metathesis transition state, but the former reaction not only is less exergonic than the latter but is also expected to be reversible, on the basis of the energy of the transition state for

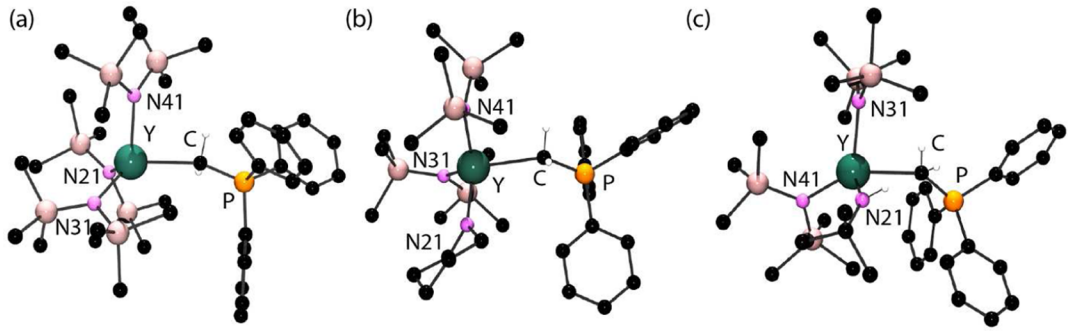

Figure 2. Crystal structures of (a) **2**·CH_2PPh_3, (b) **3a**, and (c) **3b**. Selected bond angles (deg) and bond lengths (Å): **2**·CH_2PPh_3, Y−N(21) 2.246(2), Y−N(41) 2.274(2), Y−N(31) 2.277(2), Y−C 2.554(3), C−P 1.739(3;. **3a**, Y−C 2.5441(18), P−C 1.7366(17), Y−N(21) 2.1781(15), Y−N(31) 2.2810(14), Y−N(41) 2.676(14), Y−C−P 141.33(10);**3b**, Y−C 2.531(2), P−C 1.730(2), Y−N 2.158(2), Y−N 2.273(2), Y−N 2.2633(19), Y−C−P 144.39(14).

DOI: 10.1021/acs.organomet.5b00607
Organometallics 2015, 34, 4369−4375

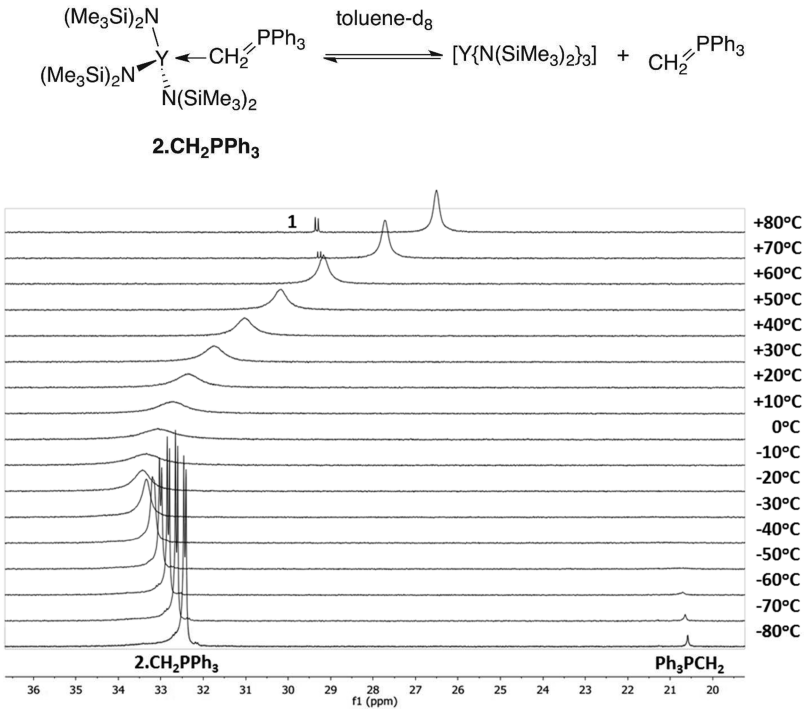

Figure 3. $^{31}P\{^{1}H\}$ NMR stack plot for a 39 mM C_7D_8 solution of **2**·CH_2PPh_3 between −80 and +80 °C.

Scheme 3. Deuterium Isotope Tracer Experiments

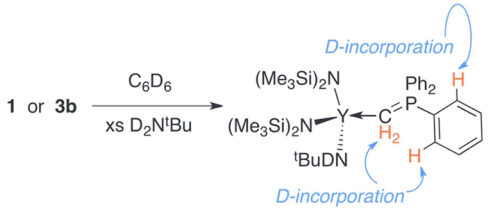

the microscopic reverse, amine elimination (Figure 4). Full details of these calculations, including the structures of the stationary points, can be found in the Supporting Information.

While we have not extended this model to more sterically demanding substrates, for hindered secondary amines the D-labeling experiments show no conclusive evidence for the addition of the amine across the aryl Y−C_{Aryl} position. Here **1** is likely to be both kinetically and thermodynamically stable with respect to the ring-opened products.

Proposed Catalytic Mechanism. To summarize the stoichiometric experiments and observations under catalytic conditions, during reactions of primary or sterically unhindered secondary amines with **1** the ylide is readily displaced from the coordination sphere of yttrium. Complexes of the form $[Y(NR_2)_3(CH_2PPh_3)]$ are potential intermediates in this reaction. In the cases where these adducts are isolable, evidence for the reversible addition of the N−H bond of the amine across *both* the Y−C_{Aryl} and Y−C_{ylide} positions of the phosphonium methylide ligand has been gathered. For sterically hindered secondary amines, no data to support the displacement of the ylide from **1** or reversible ligand activation

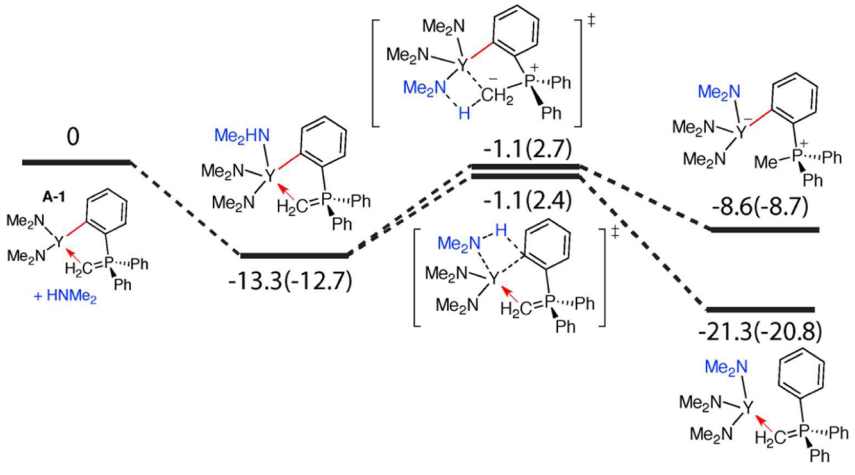

Figure 4. DFT calculations of the potential energy surfaces for addition of Me_2NH to **A-1**. Electronic energies along with solvent-corrected (PCM, benzene) energies from single-point calculations are provided. Values are given in kcal mol^{-1}. The solvent-corrected values are given in parentheses.

DOI: 10.1021/acs.organomet.5b00607
Organometallics 2015, 34, 4369−4375

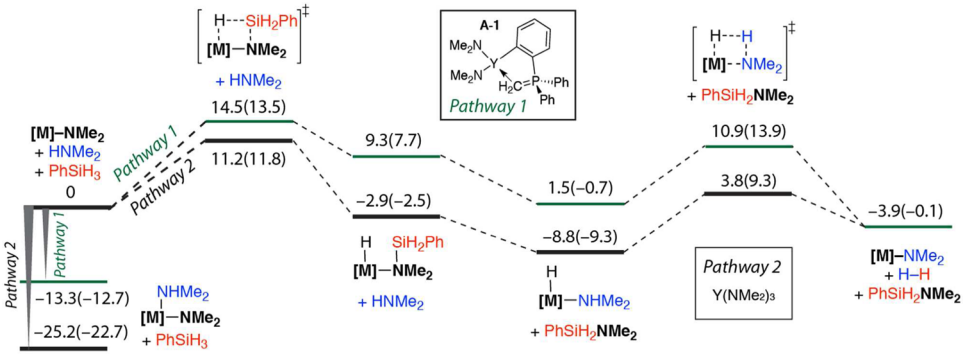

Figure 5. DFT calculations of the potential energy surface for amine–silane dehydrocoupling. Pathway 1 is catalyzed by **A-1**, and pathway 2 is catalyzed by $[Y(NMe_2)_3]$. Electronic energies along with solvent-corrected (PCM, benzene) energies from single-point calculations are provided. Values are given in kcal mol^{-1}. The solvent-corrected values are given in parentheses.

under either stoichiometric or catalytic conditions were collected.

In order to gain more insight into catalysis and to explore possible explanations for the difference between catalysts **1** and **2**, a series of DFT calculations were conducted. The potential energy surfaces for a series of reaction mechanisms for the addition of $PhSiH_3$ to Me_2NH were calculated for $[Y(NMe_2)_3]$ and **A-1** by DFT methods. To further exclude the role of ligand activation in catalysis, the conventional σ-bond metathesis pathways were compared against amine activation by addition across *both* the C_{ylide} and C_{Aryl} ligands of **A-1**. Despite repeated attempts to optimize silicate structures, there was no evidence to suggest that yttrium silicates play a role in low-energy reaction pathways. The calculated intermediates and diamond-like transition states conform to geometries that are well established in rare-earth chemistry (see the Supporting Information).[21]

The lowest energy reaction pathways occur for the addition of the amine across the Y–N bond of $[Y(NMe_2)_3]$ and the Y–N bond of **A-1** (Figure 5). While feasible reaction pathways were located for silazane formation involving amine activation using the X- or L-type ligand of **A-1**, in this model system these pathways incorporate transition states that are considerably higher in energy in comparison to those represented in Figure 5 (see the Supporting Information). These findings suggest that reversible ligand activation is not a satisfactory explanation for the improved catalytic performance of **1** over **2**. Full details of these calculations, including the structures of the stationary points, can be found in the Supporting Information.

Constitent with these theoretical data, additional deuterium labeling experiments in which **3b**, $^tBuND_2$, and $PhSiH_3$ were mixed in a 1:10:10 ratio or **1**, $^iPr_2ND$, and $PhSiH_3$ were mixed in a 1:10:10 ratio did not lead to significant D incorporation into the ortho position of the aryl group of the ligand. Hence, under catalytic conditions reversible activation of the phosphonium methylide ligand by substrate addition across the Y–C_{Aryl} bond is not significant.

The DFT studies suggest that catalytic reactions should suffer from amine inhibition, with the effect being more significant for the three-coordinate precatalyst **2** than for the four-coordinate precatalyst **1**.[22] Pathway 2 would be expected to suffer from strong catalyst inhibition due to a significant stabilization of the system upon amine coordination to $[Y(NMe_2)_3]$. Amine coordination would be expected to raise the overall activation energy to Si–N bond formation due to the need for a dissociative step prior to entering into the catalytic manifold. In contrast, pathway 1 is weakly inhibited and amine coordination to **A-1** is thermodynamically less favorable than for $[Y(NMe_2)_3]$.[23]

Although the suitability of the computational model is limited due to to the reduced size of the alkyl groups on amine and amide moieties relative to the real system, inhibition experiments in which catalytic or stoichiometric quantities of $HN(SiMe_3)_2$ were added to the reaction of $^iPr_2NH$ with $PhSiH_3$ catalyzed by **1** slowed the reaction but failed to prevent silazane formation. Under the same conditions, complex **2** shows no activity for amine silane dehydrocoupling (see Figure S5 in the Supporting Information).

Although we cannot unambigously rule out a role of the phosphorus-based ligand in supporting or solubilizing yttrium hydride clusters, we suggest that the significant difference between **1** and **2** in catalysis is a reflection of the strength of amine binding to the precatalyst and the degreee of catalyst inhibition. The difference between the two catalyst systems is borne out for the most sterically hindered amines: those which would be expected to show the largest sensitivity to the steric environment at yttrium and those for which **1** is observed as a resting state throughout the reaction.[13]

■ CONCLUSIONS

In summary, the cyclometalated complex **1** is an effective catalyst for the dehydrogenative coupling of amines and silanes. For the addition of a series of sterically demanding secondary amines to phenylsilane, this catalyst is dramatically more effective than $[Y\{N(SiMe_3)_2\}_3]$. While reversible activation of the cyclometalated ligand has been observed in stoichiometric experiments with amines, D-labeling experiments and DFT calculations suggest that reversible ligand activation is not involved in silazane formation under catalytic conditions.

■ EXPERIMENTAL SECTION

General Procedure, Exemplified for Bn_2SiH_2Ph. In a glovebox, dibenzylamine (22.4 μL, 0.12 mmol), phenylsilane (14.4 μL, 0.12 mmol), and the internal standard were dissolved in C_6D_6 (450 μL) and transferred to a Youngs tap NMR tube. The tube was removed from the glovebox, a baseline ^1H NMR spectrum was recorded, and the tube was returned to the glovebox before the addition of **3** (10 mol %) in C_6D_6 (150 μL). The reaction was monitored in situ by ^1H and ^{31}P NMR spectroscopy and gave 99% yield after 3.5 h at 25 °C. ^1H NMR (400 MHz, C_6D_6): δ 3.85 (s, 4H), 5.35 (s, 2H), 7.05–7.19 (m, 13H), 7.62–7.64 (m, 2H). ^{13}C NMR (100 MHz, C_6D_6): δ 51.2, 126.8, 128.1, 128.2, 128.3, 130.1, 134.3, 135.1, 139.8. ^{15}N NMR (51 MHz, C_6D_6): δ +24.1. ^{29}Si NMR (99 MHz, C_6D_6): δ −20.0.

DOI: 10.1021/acs.organomet.5b00607
Organometallics 2015, 34, 4369–4375

Synthesis of 2·CH_2PPh_3. In a glovebox, $[Y\{N(SiMe_3)_2\}_2]_2$ (460 mg, 0.81 mmol) and Ph_3PCH_2 (0.22 g, 0.81 mmol) were weighed out separately and transferred to a Schlenk. The Schlenk was sealed, removed from the box, and attached to a vacuum line, where dry diethyl ether (5 mL) was added under a purge of argon. The mixture was agitated and left to stand for 1 h at 25 °C. The solution was removed under vacuum, and the product was extracted into *n*-hexane (5 mL). The solution was filtered, reduced in volume, and stored at −20 °C to produce yellow crystals. The crystals were isolated through filtration and dried under vacuum to give **2**·CH_2PPh_3 (404 mg, 0.48 mmol, 59%). ^{1}H NMR (400 MHz, C_6D_6, 298 K): δ 0.45 (s, 54H), 1.23 (br d, 2H, $^2J_{^{31}P-^1H}$ = 13.6 Hz), 7.00−7.05 (m, 9H), 7.52−7.61 (m, 6H). ^{13}C NMR (101 MHz, C_6D_6, 298 K): δ 6.5, 8.5 (br), 129.0 (d, $J_{^{31}P-^{13}C}$ = 11.7 Hz), 132.4, 133.0 (d, $J_{^{31}P-^{13}C}$ = 9.7 Hz). ^{31}P NMR (162 MHz, C_6D_6, 298 K): δ + 30.5. Anal. Calcd for $C_{37}H_{71}N_3PSi_6Y$: C, 52.51; H, 8.46; N, 4.96. Found: C, 52.31, H, 8.45; N, 4.98.

Synthesis of 3a. In a glovebox, $[Y\{N(SiMe_3)_2\}_2]_2$ (400 mg, 0.70 mmol) and Ph_3PCH_2 (194 mg, 0.70 mmol) were weighed into a 20 mL scintillation vial. Dry diethyl ether (5 mL) was added, followed by piperidine (83 μL, 0.84 mmol, 1.2 equiv). The mixture was agitated and left to stand for 2 h at 25 °C. The volatiles were removed under vacuum, and the product was extracted into *n*-hexane (5 mL). The solution was filtered, reduced in volume, and stored at −20 °C to produce pale yellow crystals. The crystals were isolated through filtration and dried under vacuum to give **3a** (269 mg, 0.35 mmol, 50%). ^{1}H NMR (400 MHz, C_6D_6, 298 K): δ 0.47 (s, 36H), 1.20 (dd, 2H, $^2J^{31}$P−^{1}H = 17.6 Hz, $^2J_{^{89}Y-^1H}$ = 2.8 Hz), 1.52−1.58 (m, 4H), 1.67−1.72 (m, 2H), 3.36 (m, 4H), 7.01−7.03 (m, 9H), 7.45−7.50 (m, 6H). ^{13}C NMR (101 MHz, C_6D_6, 298 K): δ 5.8, 9.1 (dd, $^1J_{^{31}P-^{13}C}$ = $^1J_{^{89}Y-^{13}C}$ = 31.4 Hz), 27.0, 29.3, 51.9, 127.7, 128.0, 129.4 (d, $J_{^{31}P-^{13}C}$ = 11.8 Hz), 132.6 (d, $J_{^{31}P-^{13}C}$ = 2.4 Hz), 132.9 (d, $J_{^{31}P-^{13}C}$ = 9.7 Hz). ^{31}P NMR (162 MHz, C_6D_6, 298 K): δ +32.4 (d, $^2J_{^{31}P-^{89}Y}$ = 5.2 Hz). Anal. Calcd for $C_{36}H_{62}N_3PSi_4Y$: C, 56.22; H, 8.13; N, 5.46. Found: C, 56.56; H, 8.24; N, 5.40.

Synthesis of 3b. In a glovebox, $[Y\{N(SiMe_3)_2\}_2]_2$ (150 g, 0.26 mmol) and Ph_3PCH_2 (73 mg, 0.26 mmol) were weighed into a 20 mL scintillation vial. Dry diethyl ether (5 mL) was added, followed by *tert*-butylamine (33 μL, 0.32 mmol, 1.2 equiv). The mixture was agitated and left to stand for 2 h at 25 °C. The volatiles were removed under vacuum, and the product was extracted into *n*-hexane (5 mL). The solution was filtered, reduced in volume, and stored at −20 °C to produce pale yellow crystals. The crystals were isolated through filtration and dried under vacuum to give **3b** (138 mg, 0.18 mmol, 69%). ^{1}H NMR (400 MHz, C_6D_6, 298 K): δ 0.46 (s, 36H), 1.13 (dd, 2H, $^2J_{^{31}P-^1H}$ = 17.6 Hz, $^2J_{^{89}Y-^1H}$ = 2.4 Hz), 1.37 (s, 9H), 2.18 (d, 1H, $^2J_{^{89}Y-^1H}$ = 2.4 Hz), 7.01−7.04 (m, 9H), 7.52−7.58 (m, 6H). ^{13}C NMR (101 MHz, C_6D_6, 298 K): δ 6.0, 9.0 (dd, $^1J_{^{31}P-^{13}C}$ = $^1J_{^{89}Y-^{13}C}$ = 30.5 Hz), 36.2, 129.3 (d, $J_{^{31}P-^{13}C}$ = 11.8 Hz), 132.6 (d, $J_{^{31}P-^{13}C}$ = 2.4 Hz), 133.0 (d, $J_{^{31}P-^{13}C}$ = 9.7 Hz). ^{31}P NMR (162 MHz, C_6D_6, 298 K): δ +32.5 (d, $^2J_{^{31}P-^{89}Y}$ = 4.9 Hz). Due to the air-sensitive nature of this compound, repeated attempts to obtain satisfactory elemental analysis failed.

DFT Studies. Calculations were conducted in Gaussian09. All minima were confirmed by frequency calculations, and where applicable solid-state data were used as an input for the atom coordinates. Geometry optimizations were performed using the hybrid Becke three-parameter functional with Lee−Yang−Parr correlation (B3LYP). A hybrid 6,31G+(d,p) (C, H, N, Si, P) and LanL2DZ (Y) basis set was used. A (benzene) solvent correction was applied by calculating single-point energies of the optimized structures employing the polarizable continuum model in Gaussian 09.

■ ASSOCIATED CONTENT

Supporting Information

The Supporting Information is available free of charge on the ACS Publications website at DOI: 10.1021/acs.organomet.5b00607.

Full experimental and computational details and characterization data (PDF)

Computed structures (MOL)

Crystallographic data for **2**·CH_2PPh_3 and **3a**,**b** (CIF)

■ AUTHOR INFORMATION

Corresponding Author

*E-mail for M.R.C.: m.crimmin@imperial.ac.uk.

Funding

M.R.C. acknowledges the Royal Society for provision of a University Research Fellowship. A.E.N. is grateful to Imperial College London for sponsoring a Ph.D. studentship and the EPSRC for provision of a prize fellowship. We are also grateful to the Nuffield Foundation for a summer bursary for W.C.

Notes

The authors declare no competing financial interest.

■ REFERENCES

(1) Brook, M. A. *Silicon in Organic, Organometallic and Polymer Chemistry*; Wiley: Hoboken, NJ, 2000.

(2) Lekishvili, N.; Kerherashvili, M.; Lekishvili, G. *Asian J. Chem.* **2010**, *22*, 4141−4149.

(3) Grellier, M.; Ayed, T.; Barthelat, J.-C.; Albinati, A.; Mason, S.; Vendier, L.; Coppel, Y.; Sabo-Etienne, S. *J. Am. Chem. Soc.* **2009**, *131*, 7633−7640.

(4) Kocienski, P. J. *Protecting Groups*; Georg Thieme Verlag: Stuttgart, Germany, 1994.

(5) (a) Saam, J. C.; Speier, J. L. *J. Org. Chem.* **1959**, *24*, 119−120. (b) Sommer, L. H.; Citron, J. D. *J. Org. Chem.* **1967**, *32*, 2470−2472.

(6) Wang, W.-D.; Eisenberg, R. *Organometallics* **1991**, *10*, 2222−2227.

(7) (a) Blum, Y.; Laine, R. M. *Organometallics* **1986**, *5*, 2081−2086. (b) Biran, C.; Blum, Y. D.; Glaser, R.; Tse, D. S.; Youngdahl, K. A.; Laine, R. M. *J. Mol. Catal.* **1988**, *48*, 183−197. (c) Gutsulyak, D. V.; Vyboishchikov, S. F.; Nikonov, G. I. *J. Am. Chem. Soc.* **2010**, *132*, 5950−5951. (d) Konigs, C. D. F.; Müller, M. F.; Aiguabella, N.; Klare, H. F. T.; Oestreich, M. *Chem. Commun.* **2013**, *49*, 1506−1508.

(8) (a) Liu, H. Q.; Harrod, J. F. *Organometallics* **1992**, *11*, 822−827. (b) He, J.; Liu, H. Q.; Harrod, J. F.; Hynes, R. *Organometallics* **1994**, *13*, 336−343. (c) Liu, X.; Wu, Z.; Peng, Z.; Wu, Y.-D.; Xue, Z. *J. Am. Chem. Soc.* **1999**, *121*, 5350−5351. (d) Gauvin, F.; Woo, H. G. *Adv. Organomet. Chem.* **1998**, *42*, 363−405.

(9) Liu, H. Q.; Harrod, J. F. *Can. J. Chem.* **1992**, *70*, 107−110.

(10) (a) Dash, A. K.; Wang, J. X.; Berthet, J. C.; Ephritikhine, M.; Eisen, M. S. *J. Organomet. Chem.* **2000**, *604*, 83−98. (b) Wang, J. X.; Dash, A. K.; Berthet, J. C.; Ephritikhine, M.; Eisen, M. S. *J. Organomet. Chem.* **2000**, *610*, 49−57.

(11) (a) Tsuchimoto, T.; Iketani, Y.; Sekine, M. *Chem. - Eur. J.* **2012**, *18*, 9500. (b) Greb, L.; Tamke, S. *Chem. Commun.* **2014**, *50*, 2318−2320.

(12) Corriu, R. J. P.; Leclercq, D.; Mutin, P. H.; Planeix, J. M.; Vioux, A. *J. Organomet. Chem.* **1991**, *406*, C1−C4.

(13) (a) Buch, F.; Harder, S. *Organometallics* **2007**, *26*, 5132−5135. (b) Dunne, J. F.; Neal, S. R.; Engelkemier, J.; Ellern, A.; Sadow, A. D. *J. Am. Chem. Soc.* **2011**, *133*, 16782−16785. (c) Hill, M. S.; Liptrot, D. J.; MacDougall, D. J.; Mahon, M. F.; Robinson, T. P. *Chem. Sci.* **2013**, *4*, 4212−4222. (d) Bellini, C.; Carpentier, J.-F.; Tobisch, S.; Sarazin, Y. *Angew. Chem., Int. Ed.* **2015**, *54*, 7679−7683.

(14) (a) Takaki, K.; Kamata, T.; Miura, Y.; Shishido, T.; Takehira, K. *J. Org. Chem.* **1999**, *64*, 3891−3895. (c) Xie, W.; Hu, H.; Cui, C. *Angew. Chem., Int. Ed.* **2012**, *51*, 11141−11144.

(15) (a) Crimmin, M. R.; White, A. J. P. *Chem. Commun.* **2012**, *48*, 1745−1747. (b) Nako, A. E.; White, A. J. P.; Crimmin, M. R. *Chem. Sci.* **2013**, *4*, 691−695.

(16) (a) Hong, S.; Marks, T. J. *Acc. Chem. Res.* **2004**, *37*, 673−686. (b) Thompson, M. E.; Baxter, S. M.; Bulls, A. R.; Burger, B. J.; Nolan, M. C.; Santarsiero, B. D.; Schaefer, W. P.; Bercaw, J. E. *J. Am. Chem. Soc.* **1987**, *109*, 203−219.

DOI: 10.1021/acs.organomet.5b00607
Organometallics 2015, 34, 4369−4375

(17) Arnold, P. L.; McMullon, M. W.; Rieb, J.; Kühn, F. E. *Angew. Chem., Int. Ed.* **2015**, *54*, 82−100.
(18) (a) Watson, P. L.; Parshall, G. W. *Acc. Chem. Res.* **1985**, *18*, 51−56. (b) Werkema, E. L.; Messines, E.; Perrin, L.; Maron, L.; Eisenstein, O.; Andersen, R. A. *J. Am. Chem. Soc.* **2005**, *127*, 7781−7795. (c) Kefalidis, C. E.; Perrin, L.; Burns, C. J.; Berg, D. J.; Maron, L.; Andersen, R. A. *Dalton Trans.* **2015**, *44*, 2575−2587.
(19) (a) Turner, Z. R.; Bellabraba, R.; Tooze, R. P.; Arnold, P. L. *J. Am. Chem. Soc.* **2010**, *132*, 4050−4051. (b) Arnold, P. L.; Turner, Z. R.; Bellabarba, R.; Tooze, R. P. *J. Am. Chem. Soc.* **2011**, *133*, 11744−11756. (c) Arnold, P. L.; Cadenbach, T.; Marr, I. H.; Fyfe, A. A.; Bell, N. L.; Bellabarba, R.; Tooze, R. P.; Love, J. B. *Dalton Trans.* **2014**, *43*, 14346−14358.
(20) (a) Flynn, S. R.; Wass, D. F. *ACS Catal.* **2013**, *3*, 2574−2581. (b) Chapman, A. M.; Haddow, M. F.; Wass, D. F. *J. Am. Chem. Soc.* **2011**, *133*, 18463−18478. (c) Chapman, A. M.; Haddow, M. F.; Wass, D. F. *J. Am. Chem. Soc.* **2011**, *133*, 8826−8829.
(21) See for example: (a) Tobisch, S. *Dalton Trans.* **2012**, *41*, 9182−9191. (b) Maron, L.; Perrin, L.; Eisenstein, O. *J. Chem. Soc., Dalton Trans.* **2002**, 534−539.
(22) The effect of excess amine on the dielectric constant of the solvent or explicit amine solvation of the yttrium center by one or more molecules of amine was not explored at every stage of the catalytic cycle.
(23) Inhibition of pathway 2 could also occur by protonolysis and ring opening of the cyclometalated ylide with the amine (Supporting Information). On the basis of the observation of **1** as a resting state throughout the reaction with these substrates, we propose that this reaction is disfavored for sterically hindered 2° amines.

DOI: 10.1021/acs.organomet.5b00607
Organometallics 2015, 34, 4369−4375